

ABSTRACT OF THE THESIS

On Orthonormal Empirical Wavelet Bases

by

Matthew Nathan Wallace

Master of Arts in Mathematics

San Diego State University, 2025

Due to their adaptive nature, empirical wavelets have had several successes in many fields from engineering, science, medical signal/image processing. In a recent result, empirical wavelet frames were shown to be constructible by Gilles and Castro. Two natural motivations arise from this result: i. explicit construction of empirical wavelet frames for different types of wavelet kernels, ii. whether there exist orthonormal empirical wavelet bases. Both are examined in this thesis.

TABLE OF CONTENTS

	PAGE
ABSTRACT	vi
LIST OF FIGURES	viii
ACKNOWLEDGMENTS	ix
CHAPTER	
1 INTRODUCTION	1
1.1 Notation	1
1.2 Definitions	3
1.3 Partitions in the Fourier Domain	4
1.4 Foundations of Empirical Wavelet Frames	5
2 EXPLICIT CONSTRUCTION OF DISCRETE EMPIRICAL WAVELET FRAMES	7
2.1 Meyer Wavelet System	7
2.2 Littlewood-Paley Wavelet System	12
2.3 Shannon Wavelet System	15
3 NUMERICAL RESULTS	17
4 CLASSIFICATION OF EMPIRICAL ORTHONORMAL WAVELET BASES	24
5 CONCLUSION	26
BIBLIOGRAPHY	27

LIST OF FIGURES

	PAGE
2.1 Example Meyer System, Fourier Domain	9
2.2 Example Littlewood-Paley System, Fourier domain	14
3.1 Littlewood-Paley system, Fourier domain, $\beta(x) = x^4(35 - 84x + 70x^2 - 20x^3)$	20
3.2 LP Partition of Unity, $N = 50$, $\tau = \frac{1}{2}$, $\beta(x) = x$	20
3.3 Meyer System, $\beta(x) = x^4(35 - 84x + 70x^2 - 20x^3)$	22
3.4 Partition of Unity, Meyer, $\beta(x) = x^4(35 - 84x + 70x^2 - 20x^3)$	22

ACKNOWLEDGMENTS

The work presented takes a substantial amount of material from the notes of Charles-Gérard Lucas. Thank you for your work and our discussion of the Littlewood-Paley system.

CHAPTER 1

INTRODUCTION

The empirical wavelet transform was first introduced in [4], and has since shown particularly strong results in texture segmentation [9], with promising results in both time-series forecasting [12] and epileptic seizure detection [1]. Empirical wavelets share many of the same motivations as the Empirical Mode Decomposition, which was tailored to decompose a signal f into harmonic modes f_k (i.e. amplitude modulated-frequency modulated components) and some residue r :

$$f(x) = r(x) + \sum_{k=1}^N f_k(x).$$

While the Empirical Mode Decomposition was developed as a computational method, empirical wavelets have a developed mathematical framework. The purpose of empirical wavelet systems is to build a wavelet filter bank based on the supports of the modes of the original signal f . In this way, the filter bank is data-driven, as the family is dependent on the contents f . One advantage this offers over classical wavelet families is that the supports of empirical wavelets do not necessarily follow a dyadic sequence.

In [6], empirical wavelets were shown to satisfy the properties of a shift-invariant system, and using results from [8] the authors were able to show the constructability of empirical wavelet frames. The results first given in [8] have been expanded on in [3]. The work presented aims to clarify the explicit construction of empirical wavelet frames, as well as examine whether we can construct an empirical orthonormal wavelet basis for the space $L^2(\mathbb{R})$.

1.1 Notation

The used notations will be the same as in [5]. All integrals will be considered in the sense of Lebesgue. We consider the space $L^2(\mathbb{R})$ equipped with its standard inner product defined by, for all $f, g \in L^2(\mathbb{R})$,

$$\langle f, g \rangle = \int_{\mathbb{R}} f(x) \overline{g(x)} dx,$$

which induces the standard L^2 norm, i.e., for all $f \in L^2(\mathbb{R})$,

$$\|f\|_{L^2}^2 = \int_{\mathbb{R}} |f(x)|^2 dx.$$

The Fourier transform is defined, for all $f \in L^1(\mathbb{R}) \cap L^2(\mathbb{R})$, by

$$\hat{f}(\xi) = (\mathcal{F}f)(\xi) = \int_{\mathbb{R}} f(x) e^{-2\pi i \xi x} dx,$$

and its inverse by

$$f(x) = (\mathcal{F}^{-1}\hat{f})(x) = \check{\hat{f}}(x) = \int_{\mathbb{R}} \hat{f}(\xi) e^{2\pi i \xi x} d\xi.$$

The Fourier transform is classically extended to $L^2(\mathbb{R})$ as a unitary operator. Let us denote, for any arbitrary function $f \in L^2(\mathbb{R}^n)$, the following operators: translations: $T_y f(x) = f(x - y)$, where $y \in \mathbb{R}^n$; dilations: $D_a f(x) = |\det a|^{-1/2} f(a^{-1}x)$, where $a \in \mathrm{GL}_n(\mathbb{R})$; modulations: $E_\nu f(x) = e^{2\pi i \nu \cdot x} f(x)$, where $\nu \in \mathbb{R}^n$. It is straightforward to check that these operators fulfill the following properties:

$$\begin{aligned} \mathcal{F}(E_\nu f) &= T_\nu \hat{f} \quad , \quad \mathcal{F}^{-1}(T_y \hat{f}) = E_y f, \\ \mathcal{F}(T_y f) &= E_{-y} \hat{f} \quad , \quad \mathcal{F}^{-1}(E_\nu \hat{f}) = T_{-\nu} f, \\ \mathcal{F}(D_a f) &= D_{a^{-1}} \hat{f} \quad , \quad \mathcal{F}^{-1}(D_a \hat{f}) = D_{a^{-1}} f. \end{aligned}$$

When used explicitly, the Lebesgue measure will be denoted μ . Additionally, we will use the following notation for projection:

$$\mathrm{proj}_u(v) = \frac{\langle v, u \rangle}{\langle u, u \rangle} u.$$

1.2 Definitions

Definitions 1.2 - 1.4 are taken directly from [6]. Definitions listed in 1.1 are taken from [2].

Definition 1.1. A **frame** for an inner product space V is a collection $\{v_i\}_{i \in \mathcal{S}}$ such that there are constants $A, B > 0$ such that for every $u \in V$,

$$A\|u\|^2 \leq \sum_{i \in \mathcal{S}} |\langle u, v_i \rangle|^2 \leq B\|u\|^2.$$

A **tight frame** is satisfied if there exists a constant $B > 0$ such that for every $u \in V$,

$$\frac{1}{B} \sum_{i \in \mathcal{S}} |\langle u, v_i \rangle|^2 = \|u\|^2.$$

A **Parseval frame** is a tight frame of bound $B = 1$.

The strategy used in this paper to achieve an orthonormal basis relies on constructing a Parseval frame where each vector v_i is of unit norm. In that case,

$$\begin{aligned} 1 &= \sum_{i \in \mathcal{S}} |\langle v_i, v_k \rangle|^2 = \|v_k\|^4 + \sum_{i \in \mathcal{S} \setminus \{k\}} |\langle v_i, v_k \rangle|^2 \\ &\implies \langle v_i, v_k \rangle = 0 \text{ for } i \neq k \end{aligned}$$

Definition 1.2. Given a partition Ω of the frequency domain, let $\psi \in L^2(\mathbb{R})$ be a function such that its Fourier transform $\hat{\psi}$ satisfies the following two properties:

1. $\hat{\psi}$ is localized around the zero frequency,
2. There exists a subset $E \subseteq \text{supp } \hat{\psi}$ and $0 \leq \delta < 1$, such that

$$\int_E |\hat{\psi}(\xi)|^2 d\xi = (1 - \delta) \|\hat{\psi}\|_{L^2}^2.$$

This property guarantees that ψ is mostly supported by E .

Definition 1.3. An **empirical wavelet system** generated by ψ is the collection

$$\{\psi_{n,b} \mid n \in \mathcal{N}, b \in \mathbb{R}\},$$

which can be defined either in the frequency domain as

$$\forall \xi \in \mathbb{R}, \quad \hat{\psi}_{n,b}(\xi) = E_{-b} T_{\omega_n} D_{a_n} \psi(\xi) = e^{-2\pi i b \xi} \cdot |a_n|^{-1/2} \cdot \hat{\psi}\left(\frac{\xi - \omega_n}{a_n}\right), \quad (1.1)$$

or in the time domain as

$$\forall t \in \mathbb{R}, \quad \psi_{n,b}(t) = T_b E_{\omega_n} D_{1/a_n} \psi(t) = e^{2\pi i \omega_n (t-b)} \cdot |a_n|^{1/2} \cdot \psi(a_n(t-b)), \quad (1.2)$$

where ω_n is the center of the Fourier support Ω_n , and $a_n \in \mathbb{R} \setminus \{0\}$ is a scaling factor whose choice depends on Ω_n and the prototype ψ .

The notations Ω_n , ω_n used in this definition will be explained in the next section. We follow the practices of [6], and also adopt the short-hand,

$$\psi_n = E_{\omega_n} D_{1/a_n} \psi \quad \text{and} \quad \hat{\psi}_n = T_{\omega_n} D_{a_n} \hat{\psi}.$$

Thus, the full family is obtained via translation:

$$\psi_{n,b} = T_b \psi_n \quad \text{and} \quad \hat{\psi}_{n,b} = E_{-b} \hat{\psi}_n.$$

Definition 1.4. Let $b = kb_n$, where $k \in \mathbb{Z}$, and $\{b_n\}_{n \in \mathcal{N}} \subset \mathbb{R} \setminus \{0\}$. Then a **discrete empirical wavelet system** is the family of functions, for all $n \in \mathcal{N}$, $k \in \mathbb{Z}$, either defined in the Fourier domain by

$$\forall \xi \in \mathbb{R}, \quad \hat{\psi}_{n,k}(\xi) = E_{-b_n k} T_{\omega_n} D_{a_n} \psi(\xi) = e^{-2\pi i b_n k \xi} \cdot |a_n|^{-1/2} \cdot \hat{\psi}\left(\frac{\xi - \omega_n}{a_n}\right),$$

or in the time domain by

$$\forall t \in \mathbb{R}, \quad \psi_{n,k}(t) = T_{b_n k} E_{\omega_n} D_{1/a_n} \psi(t) = e^{2\pi i \omega_n (t - b_n k)} \cdot |a_n|^{1/2} \cdot \psi(a_n(t - b_n k)).$$

The corresponding discrete empirical wavelet transform is then given by

$$(E_\psi f)(n, k) = \langle f, E_{-b_n k} \psi_n \rangle = \langle f, T_{b_n k} \hat{\psi}_n \rangle.$$

Finally, a superscript is used to remind the reader of the wavelet kernel being used. We will use “LP” for Littlewood-Paley, “M” for Meyer, and “S” for Shannon.

1.3 Partitions in the Fourier Domain

Empirical wavelet systems are built from a partitioning of the Fourier domain Ω . The Fourier domain can be divided by boundaries ν_n , for $n \in \mathcal{N} \setminus \{0\} \subset \mathbb{Z}$ with $\mathcal{N} = \{n_l, \dots, n_r\}$ and $n_l, n_r \in \mathbb{Z} \cup \{-\infty, +\infty\}$, such that $\nu_n \leq 0$ if $n \leq 0$ and $\nu_n > 0$ if $n > 0$. As shown in [7], these boundaries can be obtained by way of scale-space representation. A partition $\{\Omega_n\}_{n \in \mathcal{N}}$ of the Fourier domain is a set of successive disjoint open intervals defined as

$$\Omega_n = \begin{cases} (\nu_{n-1}, \nu_n) & \text{if } n < 0, \\ (\nu_{-1}, \nu_1) & \text{if } n = 0, \\ (\nu_n, \nu_{n+1}) & \text{if } n > 0, \end{cases}$$

satisfying $\Omega = \bigcup_{n \in \mathcal{N}} \Omega_n$.

Define $\mathcal{N}_{\text{comp}} = \{n \in \mathcal{N} : \Omega_n \text{ is bounded}\}$. In the case that $\mathcal{N}_{\text{comp}} \neq \mathcal{N}$, the partition contains sets of the form $(-\infty, \nu_{n_l+1})$ and $(\nu_{n_r-1}, +\infty)$, called the left and right rays, respectively. These are discussed more extensively in [4].

While outside the focus of this thesis, for a real-valued function, the magnitude of the Fourier spectrum is even, and therefore one can consider intervals $\{\Omega_n\}_{n \in \mathcal{N}}$ built from symmetric boundaries $\nu_{-n} = \nu_n$.

1.4 Foundations of Empirical Wavelet Frames

Empirical wavelets are built on the intervals Ω_n from a wavelet kernel $\psi \in L^2(\mathbb{R})$ whose Fourier transform $\widehat{\psi}$ is localized in frequency and mostly supported on a connected open subset Λ .

Let γ_n be a continuous bijection on \mathbb{R} such that $\Lambda = \gamma_n(\Omega_n)$ if Ω_n is bounded, and $\Lambda \subsetneq \gamma_n(\Omega_n)$ otherwise. The discrete empirical wavelet system, denoted $\{\psi_n\}_{n \in \mathcal{N}}$, corresponding to the partition $\{\Omega_n\}_{n \in \mathcal{N}}$ is defined, for all $\xi \in \mathbb{R}$, by

$$\widehat{\psi}_n(\xi) = \frac{1}{\sqrt{a_n(\xi)}} \widehat{\psi} \circ \gamma_n(\xi),$$

where $a_n(\xi) > 0$ is a dilation factor that can be used for normalization. For our constructions, the mapping γ_n will be a piecewise affine function on \mathbb{R} . In this case the normalizing coefficient is defined as in [10]

$$a_n = \frac{1}{|\gamma'_n|},$$

assuming that γ_n is piecewise differentiable, to preserve that

$$\int_{\Omega_n} |\widehat{\psi}_n(\xi)|^2 d\xi = \int_E |\widehat{\psi}(\xi)|^2 d\xi.$$

In the following theorem, we denote

$$\Gamma_{comp} = \bigcup_{n \in \mathcal{N}_{comp}} \overline{\Omega_n}, \quad \mathcal{K} = \bigcup_{n \in \mathcal{N}_{comp}} b_n^{-1} \mathbb{Z}, \quad \mathcal{N}_\alpha = \{n \in \mathcal{N}_{comp} \mid b_n \alpha \in \mathbb{Z}\}.$$

In cases where Γ_{comp} is compact (or, equivalently, where $|\mathcal{N}_{comp}|$ is finite), then $\Gamma_{comp} = [\nu_m, \nu_l]$, where

$$\nu_m = \min_n \nu_n, \quad \nu_l = \max_n \nu_n.$$

For reasons that will be outlined later, we add two additional boundaries ν_{m-1} and ν_{l+1} . We then let

$$\mathcal{N}^* = \mathcal{N}_{comp} \cup \{m-1, l+1\}, \quad \mathcal{K}^* = \bigcup_{n \in \mathcal{N}^*} b_n^{-1} \mathbb{Z}, \quad \mathcal{N}_\alpha^* = \{n \in \mathcal{N}^* : b_n \alpha \in \mathbb{Z}\}.$$

If $\Gamma_{comp} = \mathbb{R}$, then we simply let

$$\mathcal{N}^* = \mathcal{N}_{comp}, \quad \mathcal{K}^* = \mathcal{K}, \quad \mathcal{N}_\alpha^* = \mathcal{N}_\alpha.$$

The case for $\Gamma_{comp} \subsetneq \mathbb{R}$, with Γ_{comp} not compact is outside the scope of our motivations.

Theorem 1.5. Let

$$L^2_{comp}(\mathbb{R}) = \{f \in L^2(\mathbb{R}) \mid \text{supp } \widehat{f} \subseteq \Gamma_{comp}\},$$

and $\Gamma_{comp} = \bigcup_{n \in \mathcal{N}_{comp}} \overline{\Omega_n}$. The system $\{T_{b_n k} \psi_n\}_{(n,k) \in \mathcal{N} \times \mathbb{Z}}$ is a Parseval frame for $L^2_{comp}(\mathbb{R})$ if and only if, for almost every $\xi \in \Gamma_{comp}$,

$$\sum_{n \in \mathcal{N}_\alpha} \frac{1}{|b_n|} \widehat{\psi}_n(\xi) \overline{\widehat{\psi}_n(\xi + \alpha)} = \delta_{\alpha,0}, \quad \text{for every } \alpha \in \mathcal{K},$$

where

$$\mathcal{K} = \bigcup_{n \in \mathcal{N}_{comp}} b_n^{-1} \mathbb{Z}, \quad \mathcal{N}_\alpha = \{n \in \mathcal{N}_{comp} \mid b_n \alpha \in \mathbb{Z}\},$$

and $\delta_{\alpha,0}$ denotes the Kronecker delta function on \mathbb{R} , i.e., $\delta_{\alpha,0} = 1$ if $\alpha = 0$, and $\delta_{\alpha,0} = 0$ otherwise.

In practice, results from **Theorem 1.5** must be split into two cases: i. global and ii. local. The global case occurs when there exists a pair b_n, b_l such that $b_n \alpha, b_l \alpha \in \mathbb{Z}$. The local case occurs when there is no such pair. In section 2.1, a proof is provided for either case for the Meyer system. In later sections, we only consider the local case.

In the following chapter we will show the explicit construction of empirical wavelet systems using three distinct wavelet kernel types: Meyer, Littlewood-Paley and Shannon. In Meyer and Littlewood-Paley, if $\Gamma_{comp} \neq \mathbb{R}$, the construction will not satisfy that

$$\sum_{n \in \mathcal{N}_\alpha} \frac{1}{|b_n|} \widehat{\psi}_n(\xi) \overline{\widehat{\psi}_n(\xi + \alpha)} = \delta_{\alpha,0}$$

for some intervals near the boundary of Γ_{comp} . We will address this in the chapter.

CHAPTER 2

EXPLICIT CONSTRUCTION OF DISCRETE EMPIRICAL WAVELET FRAMES

In this chapter we will give three examples of empirical wavelet systems and show that each satisfies a frame on $L^2_{comp}(\mathbb{R})$. Our first example is the Meyer wavelet system.

2.1 Meyer Wavelet System

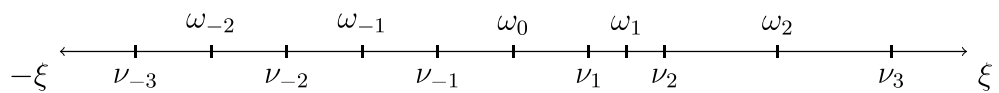
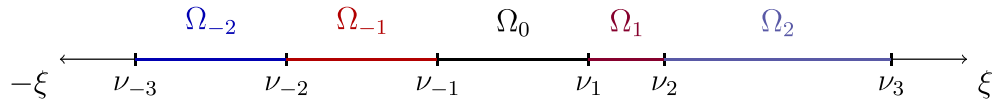
Definition 2.1. Let the 1D Meyer wavelet, compactly supported by $[-1, 1]$, be defined for $\xi \in \mathbb{R}$:

$$\hat{\psi}^M(\xi) = e^{i\frac{2\pi}{3}(\xi+1)} \begin{cases} \sin\left(\frac{\pi}{2}\beta(\xi+1)\right) & \text{if } -1 \leq \xi \leq 0, \\ \cos\left(\frac{\pi}{2}\beta(\xi)\right) & \text{if } 0 \leq \xi \leq 1, \\ 0 & \text{otherwise,} \end{cases}$$

where $\beta(x)$ is a continuous function on $[0, 1]$ such that $\beta(0) = 0$, $\beta(1) = 1$, and $\beta(x) + \beta(1-x) = 1$ for every $x \in [0, 1]$. We define γ_n such that it satisfies

$$\gamma_n : [\omega_{n-1}, \omega_{n+1}] \mapsto [-1, 1],$$

where $\omega_n = (\nu_n + \nu_{n-1})/2$ i.e. the center of the interval Ω_n . The following diagrams are given for a visual reference.



We then define

$$\gamma_n(\xi) = \begin{cases} \frac{\xi - \omega_n}{\omega_n - \omega_{n-1}} & \text{if } \xi \leq \omega_n, \\ \frac{\xi - \omega_n}{\omega_{n+1} - \omega_n} & \text{if } \xi \geq \omega_n, \end{cases}$$

To increase smoothness, the chosen function $\beta(x)$ is

$$\beta(x) = x^4(35 - 84x + 70x^2 - 20x^3).$$

Under this construction we have that

$$\|\hat{\psi}^M \circ \gamma_n\|^2 = (\omega_n - \omega_{n-1}) \int_{-1}^0 |\hat{\psi}^M(\xi)|^2 d\xi + (\omega_{n+1} - \omega_n) \int_0^1 |\hat{\psi}^M(\xi)|^2 d\xi.$$

Note that

$$\begin{aligned} 1 &= \int_0^1 \cos^2\left(\frac{\pi}{2}\beta(\xi)\right) + \int_0^1 \sin^2\left(\frac{\pi}{2}\beta(\xi)\right) \\ \implies 1 &= \int_0^1 \cos^2\left(\frac{\pi}{2}\beta(\xi)\right) + \int_0^1 \sin^2\left(\frac{\pi}{2}(1 - \beta(1 - \xi))\right) \\ \implies 1 &= 2 \int_0^1 \cos^2\left(\frac{\pi}{2}\beta(\xi)\right). \end{aligned} \tag{1}$$

This implies

$$\|\hat{\psi}^M \circ \gamma_n\|_{L^2}^2 = \frac{\omega_{n+1} - \omega_{n-1}}{2},$$

so we define

$$a_n^M(\xi) = \frac{\omega_{n+1} - \omega_{n-1}}{2}.$$

Hence, in the Fourier domain, the empirical Meyer wavelets, compactly supported by $[\omega_{n-1}, \omega_{n+1}]$, read, for every $n \in \mathcal{N}_{\text{comp}}$ and $\xi \in \mathbb{R}$,

$$\hat{\psi}_n^M(\xi) = \frac{1}{\sqrt{a_n^M(\xi)}} \hat{\psi}^M(\gamma_n(\xi)).$$

In cases where Γ_{comp} is compact (or, equivalently, where $|\mathcal{N}_{\text{comp}}|$ is finite), then $\Gamma_{\text{comp}} = [\nu_m, \nu_l]$, where

$$\nu_m = \min_n \nu_n, \quad \nu_l = \max_n \nu_n.$$

In the Meyer system,

$$\bigcup_{n \in \mathcal{N}_{\text{comp}}} \text{supp } \hat{\psi}_n^M = [\omega_{m+1}, \omega_l] \subsetneq [\nu_m, \nu_l].$$

As such, one must add two additional boundaries ν_{m-1} and ν_{l+1} . Denoting the new indexing sets as

$$\mathcal{N}^* = \mathcal{N}_{comp} \cup \{m-1, l+1\}, \quad \mathcal{K}^* = \bigcup_{n \in \mathcal{N}^*} b_n^{-1} \mathbb{Z}, \quad \mathcal{N}_\alpha^* = \{n \in \mathcal{N}^* : b_n \alpha \in \mathbb{Z}\}.$$

Then

$$\Gamma_{comp} \subset \bigcup_{n \in \mathcal{N}^*} \text{supp } \hat{\psi}_n^M.$$

This is important for bounding the Meyer frame in the global case. In the following theorem, we define \mathcal{N}^* , \mathcal{K}^* , \mathcal{N}_α^* as above if $\Gamma_{comp} \neq \mathbb{R}$, and

$$\mathcal{N}^* = \mathcal{N}_{comp}, \quad \mathcal{K}^* = \mathcal{K}, \quad \mathcal{N}_\alpha^* = \mathcal{N}_\alpha$$

otherwise. Figure 2.1 displays regions over a compact domain for which the Meyer system does not satisfy the partition of unity.

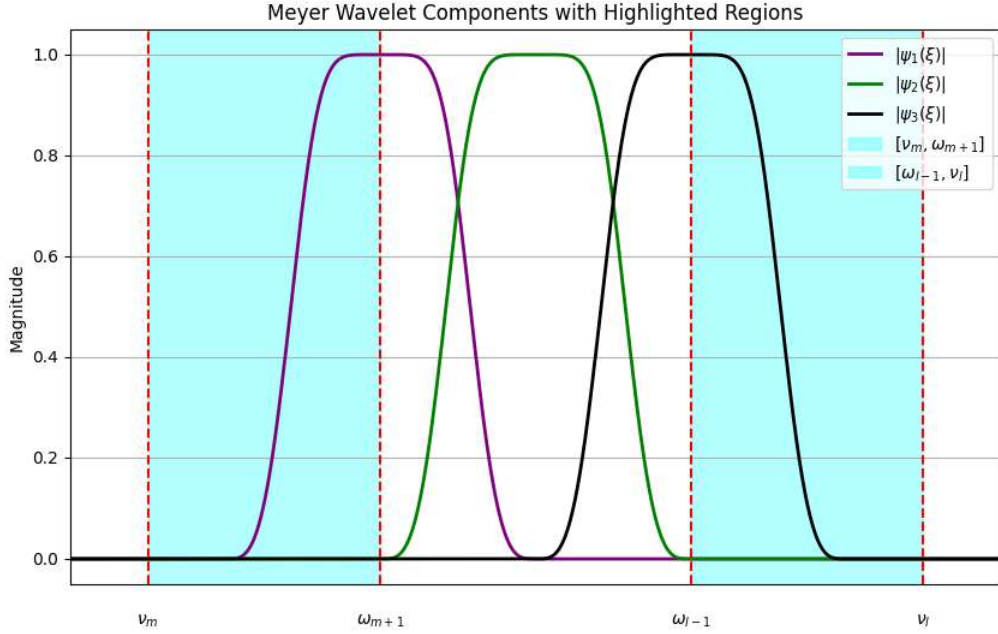


Figure 2.1. Example Meyer System, Fourier Domain

This approach is not the only way one could construct the Meyer frame. One may also note that defining

$$\begin{aligned} \hat{\psi}_{m+1}^M(\xi) &= 1 \quad \text{for } \xi \in [\nu_m, \omega_{m+1}] \\ \hat{\psi}_l^M(\xi) &= 1 \quad \text{for } \xi \in [\omega_{l-1}, \nu_l] \end{aligned}$$

allows one to apply **Theorem 1.5** without changing the indexing sets.

Theorem 2.2. *If $a_n^M = \omega_{n+1} - \omega_{n-1}$, then the system $\{T_{b_n k} \psi_n^M\}_{n \in \mathcal{N}^*, k \in \mathbb{Z}}$ is a Parseval frame on $L^2_{comp}(\mathbb{R})$ in the local case, for*

$$b_n = \frac{1}{\omega_{n+1} - \omega_{n-1}}.$$

Proof. Let $\alpha \in \mathcal{K}^* \setminus \{0\}$ and $l \in \mathcal{N}_\alpha$. There exists $j \in \mathbb{Z} \setminus \{0\}$ such that

$$j = b_l \alpha.$$

Then

$$\alpha = b_l^{-1} j = (\omega_{l+1} - \omega_{l-1}) j,$$

and it follows that

$$|\alpha| \geq \omega_{l+1} - \omega_{l-1}.$$

Then, if $\xi \in [\omega_{l-1}, \omega_{l+1}]$, we have that $\xi + \alpha \notin (\omega_{l-1}, \omega_{l+1})$, and

$$\hat{\psi}_l^M(\xi) \overline{\hat{\psi}_l^M(\xi + \alpha)} = 0.$$

Let $\alpha = 0$. For every $\xi \in \Gamma_{comp}$, there exists $n \in \mathcal{N}^*$ such that $\xi \in [\omega_n, \omega_{n+1}]$ and we have

$$\begin{aligned} \sum_{n \in \mathcal{N}_\alpha^*} \frac{1}{|b_n|} \hat{\psi}_n^M(\xi) \overline{\hat{\psi}_n^M(\xi + \alpha)} &= |\hat{\psi}_j^M(\xi)|^2 + |\hat{\psi}_{j+1}^M(\xi)|^2 \\ &= \cos^2 \left(\frac{\pi}{2} \beta \left(\frac{\xi - \omega_{j+1}}{\omega_{j+1} - \omega_j} \right) \right) + \sin^2 \left(\frac{\pi}{2} \beta \left(\frac{\xi - \omega_j}{\omega_{j+1} - \omega_j} + 1 \right) \right) \\ &= \cos^2 \left(\frac{\pi}{2} \beta \left(\frac{\xi - \omega_{j+1}}{\omega_{j+1} - \omega_j} \right) \right) + \sin^2 \left(\frac{\pi}{2} \beta \left(\frac{\xi - \omega_{j+1}}{\omega_{j+1} - \omega_j} \right) \right) \\ &= 1. \end{aligned} \tag{2}$$

Hence, for every $\alpha \in \mathcal{K}^*$ and $\xi \in \Gamma_{comp}$,

$$\sum_{l \in \mathcal{N}_\alpha^*} \frac{1}{|b_l|} \hat{\psi}_l^M(\xi) \overline{\hat{\psi}_l^M(\xi + \alpha)} = \delta_{\alpha,0},$$

which completes the proof. It is worth observing that here, $\|\hat{\psi}_n\| = \sqrt{2}$. \square

For the global case, one is forced to consider the bound over all such pairs of b_m, b_l . As we will see in the following proof, it is then important that

$$0 < \min_{n \in \mathcal{N}^*} |\omega_{n+1} - \omega_{n-1}| \leq \max_{n \in \mathcal{N}^*} |\omega_{n+1} - \omega_{n-1}| < \infty.$$

For this reason, we choose to restrict that Γ_{comp} be compact. One could choose different conditions which also guarantee the existence of these terms.

Theorem 2.3. Let Γ_{comp} be compact. The system $\{T_{b_n k} \psi_n^M\}_{(n,k) \in \mathcal{N}^* \times \mathbb{Z}}$ is a tight frame of bound $2/C$ on $L^2_{comp}(\mathbb{R})$ in the global case for

$$b_n = \frac{C}{\omega_{n+1} - \omega_{n-1}}, \quad \text{with } 0 < C \leq \frac{\min_{n \in \mathcal{N}^*} |\omega_{n+1} - \omega_{n-1}|}{\max_{n \in \mathcal{N}^*} |\omega_{n+1} - \omega_{n-1}|}$$

Proof. Let $\alpha \in \mathcal{K}$, with $\alpha \neq 0$. Let $b_j \alpha = k$ for $k \in \mathbb{Z}$. If we have that $\exists l \in \mathcal{N}_\alpha$ such that $b_l \alpha = m$. Then

$$|\alpha| = |b_j^{-1} k| = \left| \frac{\omega_{j+1} - \omega_{j-1}}{C} \right| |k|,$$

and

$$|k| = |b_j \alpha| = |b_j b_l^{-1} m| = \frac{|\omega_{l+1} - \omega_{l-1}|}{|\omega_{j+1} - \omega_{j-1}|} |m| \geq C|m|.$$

Then we have that

$$|\alpha| \geq (\omega_{j+1} - \omega_{j-1}) |m| \geq (\omega_{j+1} - \omega_{j-1}).$$

Hence if $\xi \in [\omega_{j-1}, \omega_{j+1}]$, we have that $\hat{\psi}_j^M(\xi) \overline{\hat{\psi}_j^M(\xi + \alpha)} = 0$. If $\alpha = 0$, then for every $\xi \in \Gamma_{comp}$, we have that there is a $j \in \mathcal{N}^*$ such that $\xi \in [\omega_j, \omega_{j+1}]$, we have that

$$\begin{aligned} \frac{C}{2} \sum_{n \in \mathcal{N}_\alpha^*} \frac{1}{|b_n|} \hat{\psi}_n^M(\xi) \overline{\hat{\psi}_n^M(\xi + \alpha)} &= |\psi^M \circ \gamma_n(\xi)|^2 + |\psi^M \circ \gamma_{n+1}(\xi)|^2 \\ &= 1, \end{aligned}$$

as shown in (2). Hence, we've achieved the desired result. \square

Moving on, in the next section we will construct an empirical wavelet frame with a system using a Littlewood-Paley wavelet kernel.

2.2 Littlewood-Paley Wavelet System

The Littlewood-Paley wavelet is compactly supported on $[-1, 1]$ in the Fourier domain, defined by:

$$\hat{\psi}^{LP}(\xi) = \begin{cases} \sin\left(\frac{\pi}{2}\beta(2\xi + 2)\right) & \text{if } -1 < \xi < -1/2 \\ 1 & \text{if } -1/2 \leq \xi \leq 1/2 \\ \cos\left(\frac{\pi}{2}\beta(2\xi - 1)\right) & \text{if } 1/2 < \xi \leq 1 \\ 0 & \text{otherwise} \end{cases}$$

In this case we introduce transition constants τ_n to satisfy a frame over the partition \mathcal{N} . We require that $\tau_n > 0$, with $\tau_n + \tau_{n+1} < |\Omega_n|$. As we will see later, this is chosen to satisfy the partition of unity property. Here we have that

$$\begin{aligned} \gamma_n(\xi) : [\nu_n - \tau_n, \nu_n + \tau_n] &\mapsto \left[-1, -\frac{1}{2}\right] \\ : [\nu_n + \tau_n, \nu_{n+1} - \tau_{n+1}] &\mapsto \left[-\frac{1}{2}, \frac{1}{2}\right] \\ : [\nu_{n+1} - \tau_{n+1}, \nu_{n+1} + \tau_{n+1}] &\mapsto \left[\frac{1}{2}, 1\right] \end{aligned}$$

via

$$\gamma_n(\xi) = \begin{cases} \frac{\xi - \nu_n - 3\tau_n}{4\tau_n} & \text{if } \xi \leq \nu_n + \tau_n \\ \frac{\xi - \nu_n - \tau_n}{\nu_{n+1} - \tau_{n+1} - \nu_n - \tau_n} - \frac{1}{2} & \text{if } \nu_n + \tau_n \leq \xi \leq \nu_{n+1} - \tau_{n+1} \\ \frac{\xi - \nu_{n+1} + 3\tau_{n+1}}{4\tau_{n+1}} & \text{if } \nu_{n+1} - \tau_{n+1} \leq \xi \end{cases}$$

To compute the normalizing coefficient a_n , we have the following:

$$\|\hat{\psi}_n^{LP}(\xi)\|^2 = \int_{\nu_n - \tau_n}^{\nu_n + \tau_n} |\hat{\psi}_n^{LP}(\xi)|^2 d\xi + \int_{\nu_n + \tau_n}^{\nu_{n+1} - \tau_{n+1}} |\hat{\psi}_n^{LP}(\xi)|^2 d\xi + \int_{\nu_{n+1} - \tau_{n+1}}^{\nu_{n+1} + \tau_{n+1}} |\hat{\psi}_n^{LP}(\xi)|^2 d\xi,$$

where

$$\gamma'_n(\xi) = \begin{cases} \frac{1}{4\tau_n} & \text{if } \xi \leq \nu_n + \tau_n \\ \frac{1}{\nu_{n+1} - \tau_{n+1} - \nu_n - \tau_n} & \text{if } \nu_n + \tau_n \leq \xi \leq \nu_{n+1} - \tau_{n+1} \\ \frac{1}{4\tau_{n+1}} & \text{if } \nu_{n+1} - \tau_{n+1} \leq \xi \end{cases}$$

By applying similar reasoning to what's used in (1), it can be shown that

$$\int_{-1}^{-\frac{1}{2}} |\hat{\psi}^{LP}(\xi)|^2 d\xi = \frac{1}{4},$$

$$\int_{\frac{1}{2}}^1 |\hat{\psi}^{LP}(\xi)|^2 d\xi = \frac{1}{4}.$$

We define $a_n^{LP}(\xi) = \sqrt{|\Omega_n|}$. One can verify that

$$\begin{aligned} \|\hat{\psi}_n^{LP}(\xi)\|^2 &= \int_{\nu_n - \tau_n}^{\nu_n + \tau_n} |\hat{\psi}_n^{LP}(\xi)|^2 d\xi + \int_{\nu_n + \tau_n}^{\nu_{n+1} - \tau_{n+1}} |\hat{\psi}_n^{LP}(\xi)|^2 d\xi + \int_{\nu_{n+1} - \tau_{n+1}}^{\nu_{n+1} + \tau_{n+1}} |\hat{\psi}_n^{LP}(\xi)|^2 d\xi \\ &= \frac{1}{|\Omega_n|} \left(4\tau_n \left(\frac{1}{4} \right) + |\Omega_n| - \tau_n - \tau_{n+1} + 4\tau_{n+1} \left(\frac{1}{4} \right) \right) \\ &= 1. \end{aligned}$$

Then, in the Fourier domain, the empirical Littlewood-Paley wavelets, compactly supported by $[\nu_n - \tau_n, \nu_{n+1} + \tau_{n+1}]$, read, for every $n \in \mathcal{N}_{\text{comp}}$ and $\xi \in \mathbb{R}$,

$$\hat{\psi}_n^{LP}(\xi) = \frac{1}{\sqrt{a_n^{LP}(\xi)}} (\hat{\psi}^{LP} \circ \gamma_n)(\xi).$$

Note that in this case, if Γ_{comp} is compact, then

$$\bigcup_{n \in \mathcal{N}_{\text{comp}}} \text{supp } \hat{\psi}_n^{LP} = [\nu_m - \tau_m, \nu_l + \tau_l]$$

where

$$\nu_m = \min_n \nu_n, \quad \nu_l = \max_n \nu_n.$$

However, additional boundaries ν_{m-1}, ν_{l+1} must again be placed. Without the additional boundaries, one can observe that on the intervals $[\nu_m, \nu_m + \tau_m], [\nu_l - \tau_l, \nu_l]$, the condition that

$$\sum_{n \in \mathcal{N}_\alpha} \frac{1}{|b_n|} |\hat{\psi}_n^{LP}(\xi)|^2 = 1$$

cannot be met. Figure 2.2 displays a regions over a compact domain for which the Littlewood-Paley system does not satisfy the partition of unity.

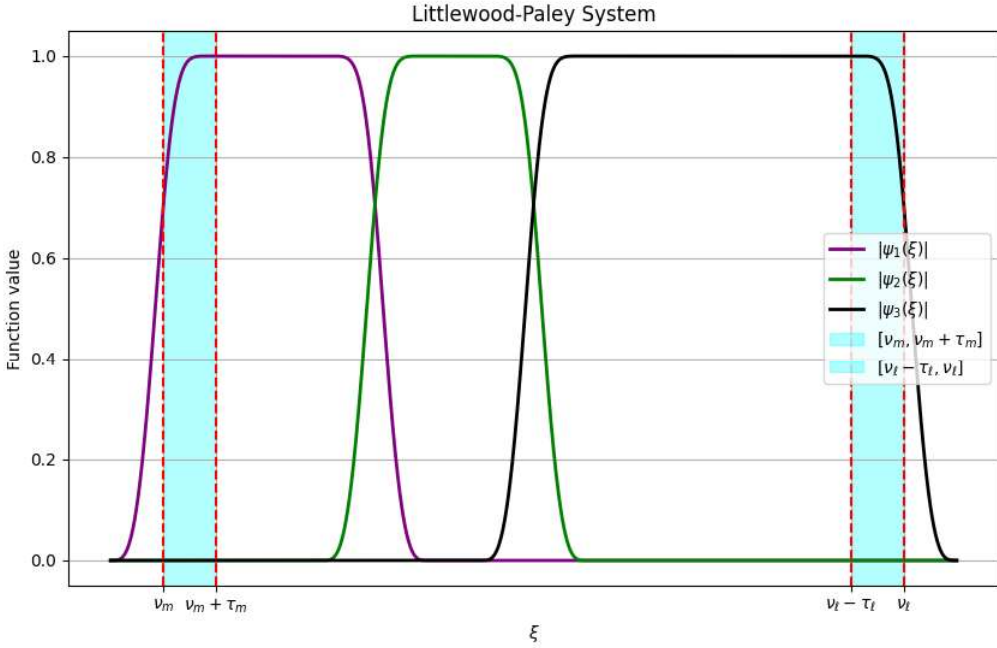


Figure 2.2. Example Littlewood-Paley System, Fourier domain

Alternatively, one can define that

$$\begin{aligned}\hat{\psi}_m^{LP}(\xi) &= 1 \quad \text{for } \xi \in [\nu_m, \nu_m + \tau_m], \\ \hat{\psi}_l^{LP}(\xi) &= 1 \quad \text{for } \xi \in [\nu_l - \tau_l, \nu_l].\end{aligned}$$

and use **Theorem 1.5** directly. We now seek to show that our system is a frame in the local case.

Theorem 2.4. Let $\Gamma_{comp} = \mathbb{R}$, with $a_n = |\Omega_n| + \tau_n + \tau_{n+1}$. The system $\{T_{b_n k} \psi_n^M\}_{(n,k) \in \mathcal{N}_{comp} \times \mathbb{Z}}$ is a tight frame of bound $1/C$ on $L^2_{comp}(\mathbb{R})$ in the local case for

$$b_n = \frac{C}{|\Omega_n| + \tau_n + \tau_{n+1}}, \quad 0 < C \leq 1$$

Proof. Let $\alpha \in \mathcal{K}$, with $\alpha \neq 0$. Let $b_j \alpha = k$ for $k \in \mathbb{Z}$. Then

$$|\alpha| = |b_j^{-1} k| = \frac{|\Omega_j| + \tau_j + \tau_{j+1}}{C} |k|$$

and therefore

$$|\alpha| \geq |\Omega_j| + \tau_j + \tau_{j+1}$$

Hence, if $\xi \in [\nu_n - \tau_n, \nu_{n+1} + \tau_{n+1}]$, we have that $\xi + \alpha \notin [\nu_n - \tau_n, \nu_{n+1} + \tau_{n+1}]$. Further, for every $\xi \in \Gamma_{comp}$ there is a $k \in \mathcal{N}$ such that $\xi \in [\nu_k - \tau_k, \nu_{k+1} + \tau_{k+1}]$. In particular, if

$\xi \in [\nu_{k+1} - \tau_{k+1}, \nu_{k+1} + \tau_{k+1}]$, then

$$\begin{aligned} C \sum_{n \in N_\alpha} \frac{1}{|b_n|} \hat{\psi}_n^{LP}(\xi) \overline{\hat{\psi}_n^{LP}(\xi + \alpha)} &= |\hat{\psi}_k^{LP}(\xi)|^2 + |\hat{\psi}_{k+1}^{LP}(\xi)|^2 \\ &= |\hat{\psi}^{LP} \circ \gamma_k(\xi)|^2 + |\hat{\psi}^{LP} \circ \gamma_{k+1}(\xi)|^2, \end{aligned}$$

the full expression of which is,

$$\begin{aligned} &= \cos^2 \left(\frac{\pi}{2} \beta \left(\frac{2(\xi - v_{k+1} + 3\tau_{k+1})}{4\tau_{k+1}} - 1 \right) \right) + \sin^2 \left(\frac{\pi}{2} \beta \left(\frac{2(\xi - v_{k+1} - 3\tau_{k+1})}{4\tau_{k+1}} + 2 \right) \right) \\ &= \cos^2 \left(\frac{\pi}{2} \beta \left(\frac{2(\xi - v_{k+1} + \tau_{k+1})}{4\tau_{k+1}} \right) \right) + \sin^2 \left(\frac{\pi}{2} \beta \left(\frac{2(\xi - v_{k+1} + \tau_{k+1})}{4\tau_{k+1}} \right) \right) \\ &= 1 \end{aligned}$$

as desired. \square

In the next section we will use a Shannon type wavelet kernel. The following system is much simpler, and under some conditions, does satisfy the properties of an orthonormal empirical wavelet basis.

2.3 Shannon Wavelet System

Define the Shannon Wavelet kernel as

$$\hat{\psi}^S(\xi) = \begin{cases} e^{i\pi(\xi+\frac{3}{2})} & \text{if } -\frac{1}{2} < \xi < \frac{1}{2} \\ 0 & \text{otherwise} \end{cases}$$

We take a natural choice of γ_n , for which

$$\gamma_n : [\nu_n, \nu_{n+1}] \mapsto [-1/2, 1/2]$$

via

$$\begin{aligned} \gamma_n(\xi) &= \frac{\xi}{|\Omega_n|} + \frac{1}{2} - \frac{\nu_{n+1}}{|\Omega_n|} \\ &= \frac{2\xi - (\nu_{n+1} + \nu_n)}{2|\Omega_n|} \\ &= \frac{\xi - \omega_n}{|\Omega_n|} \end{aligned}$$

We then define the empirical Shannon wavelet system as

$$\hat{\psi}_n^S(\xi) = \frac{1}{\sqrt{|\Omega_n|}} \hat{\psi}^S \circ \gamma_n(\xi).$$

Showing the system is a frame in the local case is straightforward.

Theorem 2.5. Let $a_n = |\Omega_n|$. The system $\{T_{b_n, k} \hat{\psi}_n^S\}$ is a tight frame on $L^2_{comp}(\mathbb{R})$ of bound $1/C$ for

$$b_n = \frac{C}{|\Omega_n|} , \quad 0 < C \leq 1$$

Proof. Let $\alpha \in \mathcal{K}$, with $\alpha \neq 0$. Let $b_j \alpha = k$ for $k \in \mathbb{Z}$. Then

$$|\alpha| = |b_j^{-1}k| = \left| \frac{|\Omega_j|}{C} \right| |k|$$

and therefore

$$|\alpha| \geq |\Omega_j|$$

Hence if $\xi \in [\nu_n, \nu_{n+1}]$, we have that $\xi + \alpha \notin (\nu_n, \nu_{n+1})$, and therefore for every $\xi \in \mathbb{R}$ we have that $\hat{\psi}^S(\xi) \overline{\hat{\psi}^S(\xi + \alpha)} = 0$. Further, we also have that for every $\xi \in \Gamma_{comp}$, there exists an $n \in \mathcal{N}$ such that $\xi \in [\nu_n, \nu_{n+1}]$, and

$$C \sum_{n \in \mathcal{N}_\alpha} \frac{1}{|b_n|} \hat{\psi}_n^S(\xi) \overline{\hat{\psi}_n^S(\xi)} = \|\psi^S\|^2 = 1$$

which completes the proof. \square

One may note that for $C = 1$, we indeed have that $\|\hat{\psi}_n^S\| = 1$. Hence, for $C = 1$, the system $\{T_{b_n, k} \hat{\psi}_n^S\}$ is an orthonormal basis for $L^2_{comp}(\mathbb{R})$.

CHAPTER 3

NUMERICAL RESULTS

Conditions to create an orthonormal basis from the Littlewood-Paley system were studied quite closely but remained unclear. This lead us to question what properties one could expect from an orthonormalized Littlewood-Paley system. Thankfully, there is at least one result which can be used to force orthogonality in the case of a finite collection of wavelets. Allowing that Γ_{comp} be compact, we may apply Gram-Schmidt to the family $\{\hat{\psi}_n^{LP}\}_{n \in \mathcal{N}_{comp}}$. First, note that the system is linearly independent, since

$$\langle \hat{\psi}_i^{LP}, \hat{\psi}_j^{LP} \rangle = 0 \quad \text{if } j \neq i \pm 1$$

and for neighboring pairs of vectors, $\hat{\psi}_i^{LP}, \hat{\psi}_{i+1}^{LP}$, we have that

$$\text{supp}\{\hat{\psi}_i^{LP}\} \neq \text{supp}\{\hat{\psi}_{i+1}^{LP}\}$$

Hence, there are no scalars $c_1, c_2 \in \mathbb{R} \setminus \{0\}$, such that

$$c_1 \hat{\psi}_i^{LP} + c_2 \hat{\psi}_{i+1}^{LP} = 0$$

We begin by fixing $\tau_n = \tau$, with $2\tau < \min_n |\Omega_n|$. Since we will compute the normalized system, here we set $a_n = 1$, where

$$\frac{1}{\sqrt{a_n^{LP}}} \hat{\psi}_n^{LP}(\xi) = \hat{\psi}^{LP} \circ \gamma_n(\xi)$$

The inner product is difficult to evaluate based on choice of β . For simplicity, if $\beta(x) = x$, then

$$\begin{aligned} \langle \hat{\psi}_n^{LP}(\xi), \hat{\psi}_{n+1}^{LP}(\xi) \rangle &= \int_{v_{n+1}-\tau}^{v_{n+1}+\tau} \cos\left(\frac{\pi}{2}(2\gamma_n(\xi) - 1)\right) \sin\left(\frac{\pi}{2}(2\gamma_{n+1}(\xi) + 2)\right) d\xi \\ &= \int_{v_{n+1}-\tau}^{v_{n+1}+\tau} \cos\left(\frac{\pi}{2}\left(\frac{\xi - \nu_{n+1}}{2\tau} + \frac{1}{2}\right)\right) \sin\left(\frac{\pi}{2}\left(\frac{\xi - \nu_{n+1}}{2\tau} + \frac{1}{2}\right)\right) d\xi \\ &= \frac{2\tau}{\pi} \left[\sin^2\left(\frac{\pi}{2}\left(\frac{\xi - \nu_{n+1}}{2\tau} + \frac{1}{2}\right)\right) \right]_{v_{n+1}-\tau}^{v_{n+1}+\tau} \\ &= \frac{2\tau}{\pi}. \end{aligned}$$

Let $|\mathcal{N}_{comp}|$ be finite, and select m such that $m - 1$ is the minimum element of \mathcal{N}_{comp} .

Re-index such that for $i \geq 1$ we replace the index $\hat{\psi}_{(m-1)+i}^{LP}(\xi)$ with $\hat{\psi}_i^{LP}(\xi)$. In other words, indexing from left to right, with the left-most wavelet denoted $\hat{\psi}_1^{LP}(\xi)$. Recall that the Gram-Schmidt process on an inner product space, V , takes a finite set of vectors $\{v_1, v_2, \dots, v_n\}$ and produces an orthogonal set $\{\tilde{e}_1, \dots, \tilde{e}_n\}$ via

$$\begin{aligned}\tilde{e}_1 &= v_1, \\ \tilde{e}_2 &= v_2 - \text{proj}_{\tilde{e}_1}(v_2), \\ &\vdots \\ \tilde{e}_n &= v_n - \sum_{k=1}^{n-1} \text{proj}_{\tilde{e}_k}(v_n).\end{aligned}$$

Finally we normalize the orthogonal vectors, with

$$\begin{aligned}e_1 &= \frac{\tilde{e}_1}{\|\tilde{e}_1\|} \\ &\vdots \\ e_n &= \frac{\tilde{e}_n}{\|\tilde{e}_n\|}\end{aligned}$$

Since $\text{supp } \hat{\psi}_i^{LP} \cap \text{supp } \hat{\psi}_j^{LP} = \emptyset$ for $|i - j| > 1$,

$$\begin{aligned}\tilde{e}_n^{LP} &= \hat{\psi}_n^{LP} - \sum_{k=1}^{n-1} \langle \hat{\psi}_n^{LP}, e_k^{LP} \rangle e_k^{LP} \\ &= \hat{\psi}_n^{LP} - \langle \hat{\psi}_n^{LP}, e_{n-1}^{LP} \rangle e_{n-1}^{LP}.\end{aligned}$$

Recall that

$$\|\hat{\psi}_{k+1}^{LP} - \text{proj}_{e_{k-1}^{LP}}(\hat{\psi}_k^{LP})\|^2 = \|\hat{\psi}_{k+1}^{LP}\|^2 - \frac{|\langle \hat{\psi}_k^{LP}, e_{k-1}^{LP} \rangle|^2}{\|e_{k-1}^{LP}\|^2},$$

and let $\rho = \frac{2\pi}{\pi}$. Then we may write the orthonormalized family $\{e_n^{LP}\}_{n \in \mathcal{N}_{comp}}$ explicitly as,

$$\begin{aligned}e_1^{LP}(\xi) &= \frac{1}{\sqrt{|\Omega_1|}} \hat{\psi}_1^{LP}(\xi), \\ e_2^{LP}(\xi) &= \frac{1}{\sqrt{|\Omega_2| - \frac{\rho^2}{|\Omega_1|}}} \left(\hat{\psi}_2^{LP}(\xi) - \frac{\rho}{\sqrt{|\Omega_1|}} e_1^{LP}(\xi) \right), \\ e_3^{LP}(\xi) &= \frac{1}{\sqrt{|\Omega_3| - \frac{\rho^2}{|\Omega_2| - \frac{\rho^2}{|\Omega_1|}}}} \left(\hat{\psi}_3^{LP}(\xi) - \frac{\rho}{\sqrt{|\Omega_2| - \frac{\rho^2}{|\Omega_1|}}} e_2^{LP}(\xi) \right),\end{aligned}$$

where the n -th orthonormalized function can be given by

$$e_n^{LP}(\xi) = \frac{1}{\sqrt{\left| \Omega_n \right| - \frac{\rho^2}{\left| \Omega_{n-1} \right| - \frac{\rho^2}{\ddots - \frac{\rho^2}{\left| \Omega_1 \right|}}}}} \left(\hat{\psi}_n^{LP}(\xi) - \frac{\rho}{\sqrt{\left| \Omega_{n-1} \right| - \frac{\rho^2}{\left| \Omega_{n-2} \right| - \frac{\rho^2}{\ddots - \frac{\rho^2}{\left| \Omega_1 \right|}}}}} e_{n-1}^{LP}(\xi) \right).$$

While this achieves an orthonormal set, the Gram-Schmidt process introduces ‘leakage,’ where

$$\text{supp}(e_1^{LP}) \subset \text{supp}(e_2^{LP}) \subset \dots \subset \text{supp}(e_n^{LP}).$$

And, on closer inspection, the partition of unity property is not respected.

However, for the usual choice, $\beta(x) = x^4(35 - 84x + 70x^2 - 20x^3)$, the integral must be evaluated numerically. In this case we have that

$$\begin{aligned} \langle \hat{\psi}_n^{LP}(\xi), \hat{\psi}_{n+1}^{LP}(\xi) \rangle &= \int_{v_{n+1}-\tau}^{v_{n+1}+\tau} \cos\left(\frac{\pi}{2}\beta(2\gamma_n(\xi) - 1)\right) \sin\left(\frac{\pi}{2}\beta(2\gamma_{n+1}(\xi) + 2)\right) d\xi \\ &= 2\tau \int_0^1 \cos\left(\frac{\pi}{2}\beta(\xi)\right) \sin\left(\frac{\pi}{2}\beta(\xi)\right) d\xi \\ &= 2\tau M \end{aligned}$$

with $M \approx 0.17886\dots$. Letting $\rho = 2\tau M$, the previous Gram-Schmidt formulas hold.

Figure 3.1 displays the Gram-Schmidt process in the Fourier domain. Figure 3.2 displays the partition of unity property after performing Gram-Schmidt on the Littlewood-Paley system.

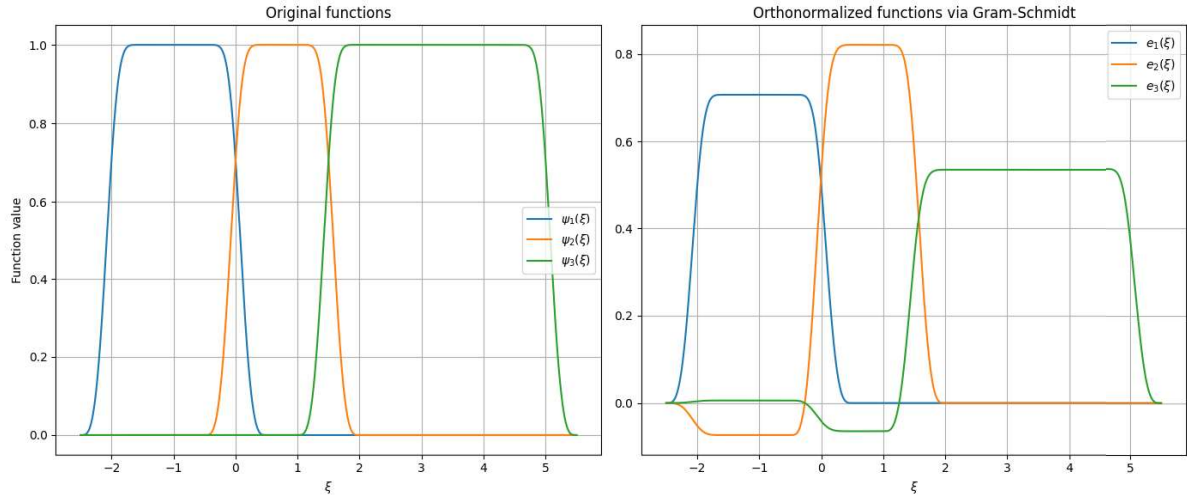


Figure 3.1. Littlewood-Paley system, Fourier domain, $\beta(x) = x^4(35 - 84x + 70x^2 - 20x^3)$

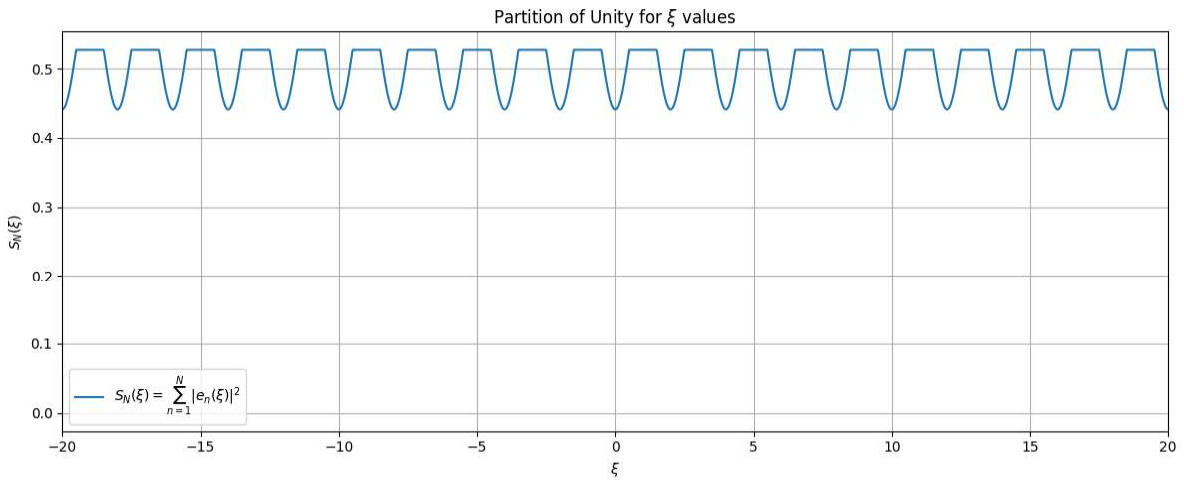


Figure 3.2. LP Partition of Unity, $N = 50$, $\tau = \frac{1}{2}$, $\beta(x) = x$

For the Meyer system, the Gram-Schmidt process also distorts the structure of the supports. Due to having more variation in overlapping supports, we instead give a recursive formula to perform the Gram-Schmidt process. This time, we take

$$\frac{1}{a_n} = \frac{2}{\omega_{n+1} - \omega_{n-1}} , \quad \beta(x) = x^4(35 - 84x + 70x^2 - 20x^3)$$

and re-index as previously given. Then

$$\begin{aligned} \langle \hat{\psi}_n^M, \hat{\psi}_{n+1}^M \rangle &= \frac{1}{\sqrt{a_n a_{n+1}}} \int_{\omega_n}^{\omega_{n+1}} \cos\left(\frac{\pi}{2}\beta\left(\frac{\xi - \omega_{n+1}}{\omega_{n+1} - \omega_n}\right)\right) \sin\left(\frac{\pi}{2}\beta\left(\frac{\xi - \omega_{n+1}}{\omega_{n+1} - \omega_n}\right)\right) d\xi \\ &= \frac{(\omega_{n+1} - \omega_n)}{\sqrt{a_n a_{n+1}}} \int_{-1}^0 \cos\left(\frac{\pi}{2}\beta(\xi)\right) \sin\left(\frac{\pi}{2}\beta(\xi)\right) d\xi \\ &= \frac{(\omega_{n+1} - \omega_n)}{\sqrt{a_n a_{n+1}}} \cdot L, \end{aligned}$$

where

$$L \approx 0.04182\dots$$

Let

$$\rho_n = \langle \hat{\psi}_n^M, \hat{\psi}_{n-1}^M \rangle = \frac{(\omega_n - \omega_{n-1})}{\sqrt{a_n a_{n-1}}} L,$$

and

$$r_n = \langle \hat{\psi}_n^M, e_{n-1}^M \rangle.$$

Then we have that

$$r_n = \langle \hat{\psi}_n^M, \frac{\hat{\psi}_{n-1}^M - r_{n-1} e_{n-2}^M}{\sqrt{1 - |r_{n-1}|^2}} \rangle.$$

By linearity of the inner product, noting again that

$$\langle \hat{\psi}_i^M, \hat{\psi}_j^M \rangle = 0 \text{ if } j \neq i \pm 1,$$

we have that

$$\begin{aligned} r_n &= \frac{\langle \hat{\psi}_n^M, \hat{\psi}_{n-1}^M \rangle}{\sqrt{1 - |r_{n-1}|^2}} \\ &= \frac{\rho_n}{\sqrt{1 - |r_{n-1}|^2}}. \end{aligned}$$

Then

$$r_1 = 0, \quad r_2 = \rho_2, \quad r_n = \frac{\rho_n}{\sqrt{1 - |r_{n-1}|^2}} \text{ for } n \geq 3.$$

Thus, $e_1^M = \hat{\psi}_1^M$, and for $n > 1$:

$$e_n^M = \frac{\hat{\psi}_n^M - r_n e_{n-1}^M}{\sqrt{1 - |r_{n-1}|^2}}.$$

Figure 3.3 displays the Gram-Schmidt process on the Meyer system in the Fourier domain. Figure 3.4 displays the partition of unity property after performing Gram-Schmidt on the Meyer system.

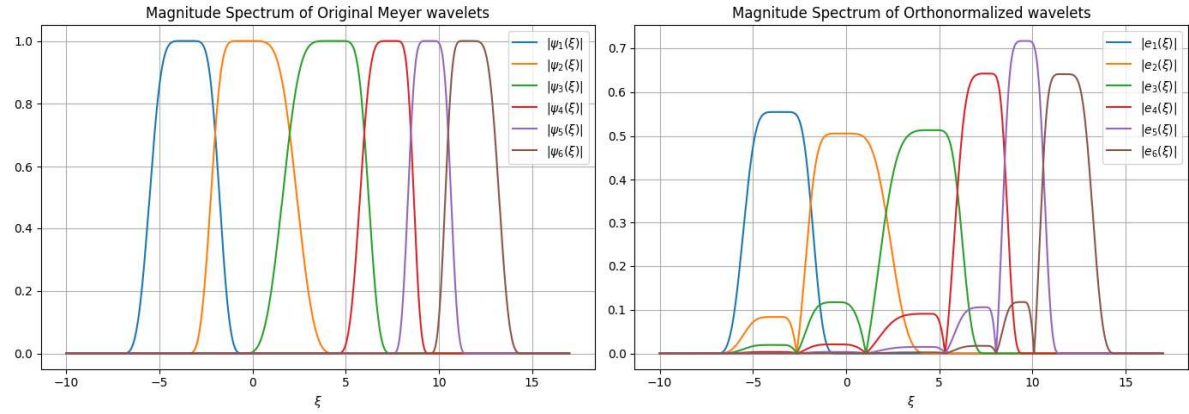


Figure 3.3. Meyer System, $\beta(x) = x^4(35 - 84x + 70x^2 - 20x^3)$

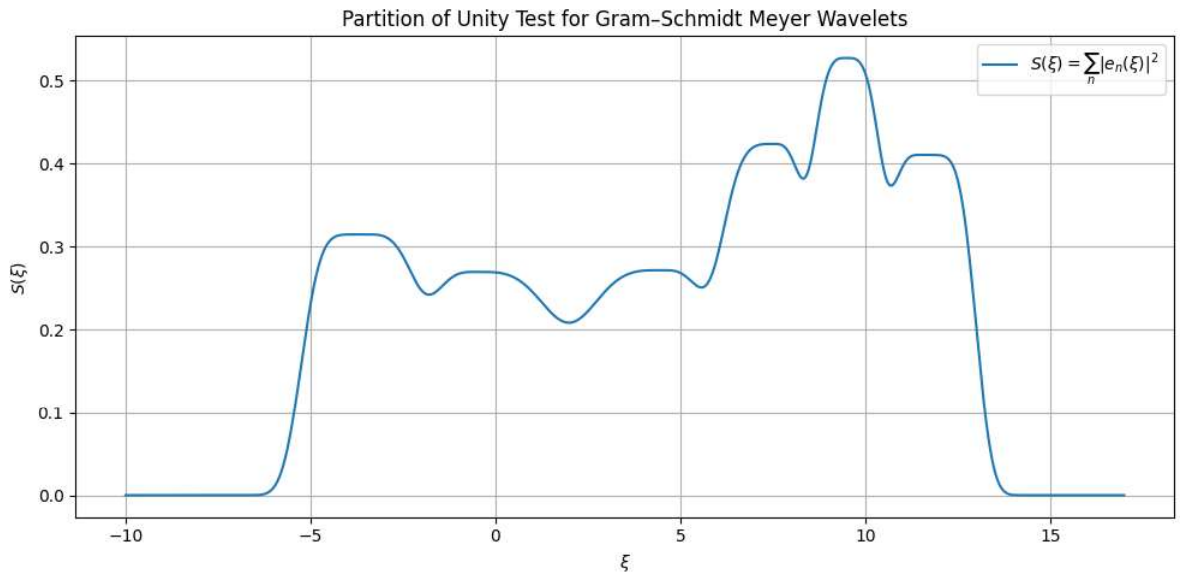


Figure 3.4. Partition of Unity, Meyer, $\beta(x) = x^4(35 - 84x + 70x^2 - 20x^3)$

As we can see, while the achieved set of functions is orthonormal, the partition of unity property is lost as a result. As a consequence, in the next chapter we revisit what properties one can expect from an orthonormal empirical wavelet system without consideration to the wavelet kernel used.

CHAPTER 4

CLASSIFICATION OF EMPIRICAL ORTHONORMAL WAVELET BASES

Since forcing orthogonality in using the Gram-Schmidt algorithm did not lead to further insights, instead we turn our attention to what characteristics one can expect from an orthonormalized empirical wavelet system. In this chapter, we will show that if $\{T_{b_n k} \psi_n\}_{(n,k) \in \mathcal{N}_{comp} \times \mathbb{Z}}$ satisfies an orthonormal basis of $L^2_{comp}(\mathbb{R})$, then for a.e. $\xi \in \Gamma_{comp}$

$$\frac{1}{|b_n|} |\hat{\psi}_n(\xi)|^2 = \chi_{S_n}(\xi),$$

where $S_n = \text{supp } \psi_n$. We will show this by using the following lemma, where our proof strategy is to simply use **Theorem 1.5** in reverse.

Lemma 4.1. *Any discrete empirical wavelet system where*

$$\mu(\text{supp } \hat{\psi}_n \cap \text{supp } \hat{\psi}_{n+1}) \neq 0$$

cannot satisfy an orthonormal basis of $L^2_{comp}(\mathbb{R})$.

Proof. Let the system $\{T_{b_n k} \psi_n\}_{(n,k) \in \mathcal{N}_{comp} \times \mathbb{Z}}$ satisfy an orthonormal basis of $L^2_{comp}(\mathbb{R})$. Necessarily the system must be a Parseval frame of $L^2_{comp}(\mathbb{R})$, and satisfy that

$$\|\hat{\psi}_n\|^2 = 1. \tag{3}$$

Using **Theorem 1.5**, it is required that for every $\alpha \in \mathcal{K} \setminus \{0\}$,

$$\frac{1}{|b_n|} \hat{\psi}_n(\xi) \overline{\hat{\psi}_n(\xi + \alpha)} = 0$$

for almost every $\xi \in \Gamma_{comp}$. One can observe that by fixing $l \in \mathcal{N}_{comp}$, for $\alpha = b_l^{-1} \in \mathcal{K} \setminus \{0\}$, we must have that for almost every $\xi \in \Gamma_{comp}$

$$\hat{\psi}_l(\xi) \overline{\hat{\psi}_l(\xi + b_l^{-1})} = 0,$$

which is only true if

$$\frac{1}{|b_l|} \geq \mu(\text{supp } \hat{\psi}_l).$$

Let

$$J = \text{supp } \hat{\psi}_n \cup \text{supp } \hat{\psi}_{n+1}, \quad I = \text{supp } \hat{\psi}_n \cap \text{supp } \hat{\psi}_{n+1}.$$

Using (3)

$$\begin{aligned} \int_J \frac{1}{|b_n|} |\hat{\psi}_n(\xi)|^2 + \frac{1}{|b_{n+1}|} |\hat{\psi}_{n+1}(\xi)|^2 d\xi &= \frac{1}{|b_n|} \|\hat{\psi}_n\|^2 + \frac{1}{|b_{n+1}|} \|\hat{\psi}_{n+1}\|^2 \\ &= \frac{1}{|b_n|} + \frac{1}{|b_{n+1}|} \\ &\geq \mu(\text{supp } \hat{\psi}_n) + \mu(\text{supp } \hat{\psi}_{n+1}). \end{aligned}$$

However, on J ,

$$\frac{1}{|b_n|} |\hat{\psi}_n(\xi)|^2 + \frac{1}{|b_{n+1}|} |\hat{\psi}_{n+1}(\xi)|^2 \leq 1.$$

Hence we have that

$$\int_J \frac{1}{|b_n|} |\hat{\psi}_n(\xi)|^2 + \frac{1}{|b_{n+1}|} |\hat{\psi}_{n+1}(\xi)|^2 d\xi \leq \mu(J).$$

This implies

$$\frac{1}{|b_n|} + \frac{1}{|b_{n+1}|} \leq \mu(J).$$

Combining both inequalities gives

$$\begin{aligned} \mu(\text{supp } \hat{\psi}_n) + \mu(\text{supp } \hat{\psi}_{n+1}) &\leq \frac{1}{|b_n|} + \frac{1}{|b_{n+1}|} \leq \mu(J) \\ \mu(\text{supp } \hat{\psi}_n) + \mu(\text{supp } \hat{\psi}_{n+1}) &\leq \frac{1}{|b_n|} + \frac{1}{|b_{n+1}|} \leq \mu(\text{supp } \hat{\psi}_n) + \mu(\text{supp } \hat{\psi}_{n+1}) - \mu(I) \\ \implies \mu(I) &= 0. \end{aligned}$$

□

By **Lemma 4.1**, since any candidate system must have the restriction that

$$\mu(\text{supp } \hat{\psi}_n \cap \text{supp } \hat{\psi}_{n+1}) = 0,$$

in this case, for a.e. $\xi \in \Gamma_{comp}$, $\exists! l \in \mathcal{N}$ such that $\xi \in \text{supp } \hat{\psi}_l$, and

$$\sum_{n \in \mathcal{N}_\alpha} \frac{1}{|b_n|} |\hat{\psi}_n(\xi)|^2 = \frac{1}{|b_l|} |\hat{\psi}_l(\xi)|^2 = 1.$$

Hence we've shown the result.

CHAPTER 5

CONCLUSION

Sections 1.3 and 1.4 are taken directly from the notes of Dr. Charles-Gerard Lucas. Additionally in Chapter 2 we gave some results on empirical wavelet frames over a compact domain Γ_{comp} . The proofs that these systems are frames over the full domain $L^2(\mathbb{R})$ were developed by Dr. Lucas. The remaining chapters contain original results from the author. While each chapter aimed to clarify the conditions for orthogonal empirical wavelet bases, there remain further topics worthy of investigation. The main result shown in Chapter 4 narrows the possible choices for empirical wavelet systems satisfying an orthonormal basis, however is not as illuminating as one would hope. There are two natural extensions of the work presented which warrant further study: i. the extension of the work given to higher-dimensional systems (as given in recent work [10], the partitioning required for the empirical wavelet transform in \mathbb{R}^n comes with some constraints for $n > 1$), and ii. the development of more sophisticated machinery in the analysis of empirical wavelet bases. For example, the Zak transform is demonstrably one of the most powerful tools in the analysis of Gabor bases, revealing many of the qualifying properties which would otherwise be very difficult to prove [2]. Whether there exists an equally potent transform for shift-invariant systems is perhaps the strongest result one could look for.

BIBLIOGRAPHY

- [1] A. BHATTACHARYYA, V. GUPTA, AND R. B. PACHORI, *Automated identification of epileptic seizure EEG signals using empirical wavelet transform based Hilbert marginal spectrum*, in Proceedings of the 22nd International Conference on Digital Signal Processing (DSP), 2017, <https://doi.org/10.1109/icdsp.2017.8096122>.
- [2] O. CHRISTENSEN, *An Introduction to Frames and Riesz Bases*, Applied and Numerical Harmonic Analysis, Birkhäuser, Basel, 2016, <https://doi.org/10.1007/978-3-319-25613-9>.
- [3] O. CHRISTENSEN, M. HASANNASAB, AND J. LEMVIG, *Explicit constructions and properties of generalized shift-invariant systems in $l^2(\mathbb{R})$* , Advances in Computational Mathematics, 43 (2017), pp. 443–472, <https://doi.org/10.1007/s10444-016-9492-x>.
- [4] J. GILLES, *Empirical wavelet transform*, IEEE Transactions on Signal Processing, 61 (2013), pp. 3999–4010, <https://doi.org/10.1109/TSP.2013.2265222>.
- [5] J. GILLES, *Continuous empirical wavelets systems*, Advances in Data Science and Adaptive Analysis, 12 (2020), p. 2050006, <https://doi.org/10.1142/S2424922X20500063>.
- [6] J. GILLES AND R. CASTRO, *Empirical wavelet frames*, Advances in Data Science and Adaptive Analysis, 17 (2025), p. 2550001, <https://doi.org/10.1142/S2424922X25500019>.
- [7] J. GILLES AND K. HEAL, *A parameterless scale-space approach to find meaningful modes in histograms—application to image and spectrum segmentation*, International Journal of Wavelets, Multiresolution and Information Processing, 12 (2014), p. 1450044, <https://doi.org/10.1142/S0219691314500446>.
- [8] E. HERNÁNDEZ, D. LABATE, AND G. WEISS, *A unified characterization of reproducing systems generated by a finite family, ii*, Journal of Geometric Analysis, 12 (2002), pp. 615–662, <https://doi.org/10.1007/BF02930656>.
- [9] B. HURAT, Z. ALVARADO, AND J. GILLES, *The empirical watershed wavelet*, Journal of Imaging, 6 (2020), p. 140, <https://doi.org/10.3390/jimaging6120140>.
- [10] C.-G. LUCAS AND J. GILLES, *Multidimensional empirical wavelet transform*, SIAM Journal on Imaging Sciences, 18 (2025), pp. 906–935, <https://doi.org/10.1137/24M1659613>.
- [11] Y. MEYER, *Wavelets and Operators*, vol. 37 of Cambridge Studies in Advanced Mathematics, Cambridge University Press, 1993, <https://doi.org/10.1017/CBO9780511623820>.

- [12] H. A. MOHAMMADI, S. GHOFRANI, AND A. NIKSERESHT, *Using empirical wavelet transform and high-order fuzzy cognitive maps for time series forecasting*, Applied Soft Computing, 135 (2023), p. 109990,
<https://doi.org/10.1016/j.asoc.2023.109990>.